Research Article

Chu Cheng*, Ziwei Song, Lingfeng Wang, Long Zhao, Lisha Wang, Linfang Guo, Bowen Shi, and Kexing Song*

Effects of microalloying elements added by *in situ* synthesis on the microstructure of WCu composites

https://doi.org/10.1515/ntrev-2022-0045
received December 31, 2021; accepted January 15, 2022

Abstract: The addition of microalloying elements improves the microstructure and properties of copper-based materials. In this study, WCu composites are synthesized *in situ* with Fe, Ni, or Mn as microalloying elements, and the effects of each element on the microstructural characteristics of the obtained composite are investigated. Fe, Ni, and Mn can be added *in situ* to WCu composites by thermite reduction. Increasing the temperature is not conducive to the reduction of MnO_2 by Al. Ni, Fe, and Mn were well dissolved in the copper matrix, and their contents decreases in turn, while the Al content in the matrix increases in turn. Mn clearly reduces the size of tungsten particles, and the size reduction effect of the microalloying elements on tungsten particles follows the order Mn > Fe > Ni. The effect on the wettability of the interface follows the order Ni > Mn > Fe. Increasing the interfacial wetting is not conducive to the refinement of tungsten particles.

Keywords: WCu composite, microalloying element, thermite reduction

*** Corresponding author: Chu Cheng,** School of Materials Science and Engineering, Henan University of Science and Technology, Luoyang 471023, China; Provincial and Ministerial Co-construction Collaborative Innovation Center of Nonferrous New Materials and Advanced Processing Technology, Luoyang 471023, China; Henan Key Laboratory of Advanced Non-Ferrous of Metals, Luoyang 471023, China, e-mail: cheng_chu_love@126.com
*** Corresponding author: Kexing Song,** Provincial and Ministerial Co-construction Collaborative Innovation Center of Nonferrous New Materials and Advanced Processing Technology, Luoyang 471023, China, e-mail: kxsong123@163.com
Ziwei Song: School of Materials Science and Engineering, Henan University of Science and Technology, Luoyang 471023, China, e-mail: s18236378861@163.com
Lingfeng Wang: School of Materials Science and Engineering, Henan University of Science and Technology, Luoyang 471023, China, e-mail: wlf18339326802@163.com
Long Zhao: School of Materials Science and Engineering, Henan University of Science and Technology, Luoyang 471023, China, e-mail: zl2259667209@163.com
Lisha Wang: School of Materials Science and Engineering, Henan University of Science and Technology, Luoyang 471023, China, e-mail: wls6291@163.com
Linfang Guo: School of Materials Science and Engineering, Henan University of Science and Technology, Luoyang 471023, China, e-mail: 18790733920@163.com
Bowen Shi: School of Materials Science and Engineering, Henan University of Science and Technology, Luoyang 471023, China, e-mail: shibowen1002021@163.com

1 Introduction

Tungsten/copper (WCu) composites have the advantages of high density, high strength, high hardness, good electrical and thermal conductivity, and arc erosion resistance [1–3]. They are widely used in electrical contacts for high-voltage switches, resistance welding electrodes, aerospace rocket nozzles, *etc.* [4,5]. Because of the large differences in melting point and solubility between W and Cu, WCu is usually fabricated by powder metallurgy using superfine metal powders as raw materials [6]. However, because tungsten and copper are immiscible, the strength and density of WCu fabricated by powder metallurgy cannot meet the requirements for the rapid development of electrical contacts for high-voltage switches, resistance welding electrodes, and aerospace rocket nozzles [7–9].

Microalloying improves the mechanical properties of copper alloys [10]. Many researchers worldwide have investigated methods of improving the density and strength of WCu composites by adding microalloying elements [11–15]. Johnson and Cao [16,17] researched the effect of Fe and Co on the properties of WCu alloys. They found that a finite solid solution with Cu could be produced by adding small amounts of Fe and Co as activated elements during sintering, and the second phase can precipitate, producing intermetallic compounds at grain boundaries, which can promote the densification of tungsten and clearly improve the density of WCu composites. Yang *et al.* [18] studied the effect of alloying with Ni and Cr on the wettability of Cu on a W substrate. The results indicated that the wettability of liquid copper on a W substrate is distinctly improved by adding Cr and Ni, and interfacial metallurgic bonding is realized by the mutual diffusion and dissolution of various elements at the interface. Wang and Liang [19,20] investigated the interface microstructure of a novel WCu/Al composite fabricated by an infiltration method. They found that five transition zones formed at the WCu/Al interface, specifically, layer-like, hypereutectic, eutectic, hypoeutectic, and needle-like zones, from the WCu side to the Al side. In summary, the addition of microalloying elements improves the wettability of the WCu interface, which further improves the density and strength of WCu composites. The conventional powder metallurgy methods can be classified as infiltration processes and high-temperature sintering [21,22]. In infiltration processes, microalloying elements are first added to liquid copper to form a copper alloy, which is infiltrated into the tungsten skeleton [23]. In high-temperature sintering, microalloying elements are added as metal powders; thus, the microalloying elements are often unevenly distributed because of uneven mixing [24,25].

Based on our previous studies [26–30], a novel method of synthesizing microalloyed WCu composites by aluminothermic reduction has been proposed. In this study, WO_3, CuO, and Al powder and microalloying element oxides are used as raw materials to induce the self-propagating high-temperature synthesis (SHS) reaction, during which micro- and nanosized tungsten particles, liquid copper, and microalloying element particles are produced by *in situ* synthesis. To produce low-melting-point calcium aluminates, CaO is used as slag formers, which is combined with the generated Al_2O_3. After the SHS reaction, the metal and slag are phase-separated owing to differences in density; finally, a microalloyed WCu composite ingot is obtained. The microalloying element added by *in situ* synthesis are more uniformly distributed in WCu composites than that added by powder metallurgy. The thermodynamic equilibria of the Al–CuO–WO_3–Fe_2O_3/NiO/MnO_2 systems are calculated. WCu composites microalloyed with Fe, Ni, or Mn are synthesized *in situ*, and the effects of the microalloying elements on the microstructural characteristics of the WCu composites are investigated. This study provides a theoretical basis for the preparation of homogeneous high-density WCu composites.

2 Experiment

2.1 Materials

WO_3 (99.90 wt%, particle size: 80–100 nm), Fe_2O_3 (99.50 wt%, particle size: ≤0.20 mm), NiO (99.80 wt%, particle size: ≤0.20 mm), MnO_2 (99.50 wt%, particle size: ≤0.20 mm), and CuO (99.50 wt%, particle size: ≤0.20 mm) were used as raw materials. CuO was obtained from Zhengzhou Baixiang Chemical Reagent Co., Ltd., China, and WO_3, Fe_2O_3, MnO_2, and NiO were obtained from Sinopharm Chemical Reagent Co., Ltd., China. Aluminum powder (99.5% pure, particle diameter: 0.1–3 mm) was used as a reductant. CaO (99.50% pure, particle diameter: ≤0.25 mm) and magnesium powder (99.5% pure, particle diameter: ≤0.2 mm) were supplied by Sinopharm Chemical Reagent Co., Ltd., China.

2.2 Experimental methods and analysis

The experiment was conducted under atmospheric pressure to synthesize WCu composites containing 3.0 wt% of each microalloying element. To prepare the raw materials before synthesis, Fe_2O_3, NiO, MnO_2, WO_3, CuO, and CaO were heated in air at 573 K for 24 h to remove water. The raw materials were weighed in desired proportions and placed in a ball mill. The total mass of materials in each experiment was about 2 kg. The tank was covered with a lid, and the reagents were mixed using a can mixer for 60 min. Then, they were placed in a conical graphite reactor enclosed by a magnesia lining with a volume of 10 L. Approximately 2–3 g of Mg powder was used as an easy ignition agent and placed on top of the other reagents. Mg powder was ignited to induce SHS and obtain a high-temperature melt. Next, the melt was cast in a graphite crucible and cooled to approximately 298 K.

2.3 Calculation and analysis methods

The adiabatic temperature (T_{ad}) and thermodynamic equilibrium of the Al–CuO–WO_3–Fe_2O_3, Al–CuO–WO_3–NiO, and Al–CuO–WO_3–MnO_2 systems were calculated by HSC 6.0. The chemical compositions of the microalloyed WCu composites were analyzed by inductively coupled plasma emission spectrometry (Optima 4300DV, Lehman, USA), and their oxygen content was measured using an oxygen/nitrogen/hydrogen analyzer (Type G8, Bruker, Germany). Samples of the composite ingots and slag were characterized using scanning electron microscopy (SEM) coupled with energy-dispersive X-ray spectroscopy (EDS; SU-8010, Hitachi, Japan).

3 Results and discussion

3.1 Thermodynamics

The adiabatic temperatures (T_{ad}) of the Al–CuO–WO_3–Fe_2O_3, Al–CuO–WO_3–NiO, and Al–CuO–WO_3–MnO_2 systems were

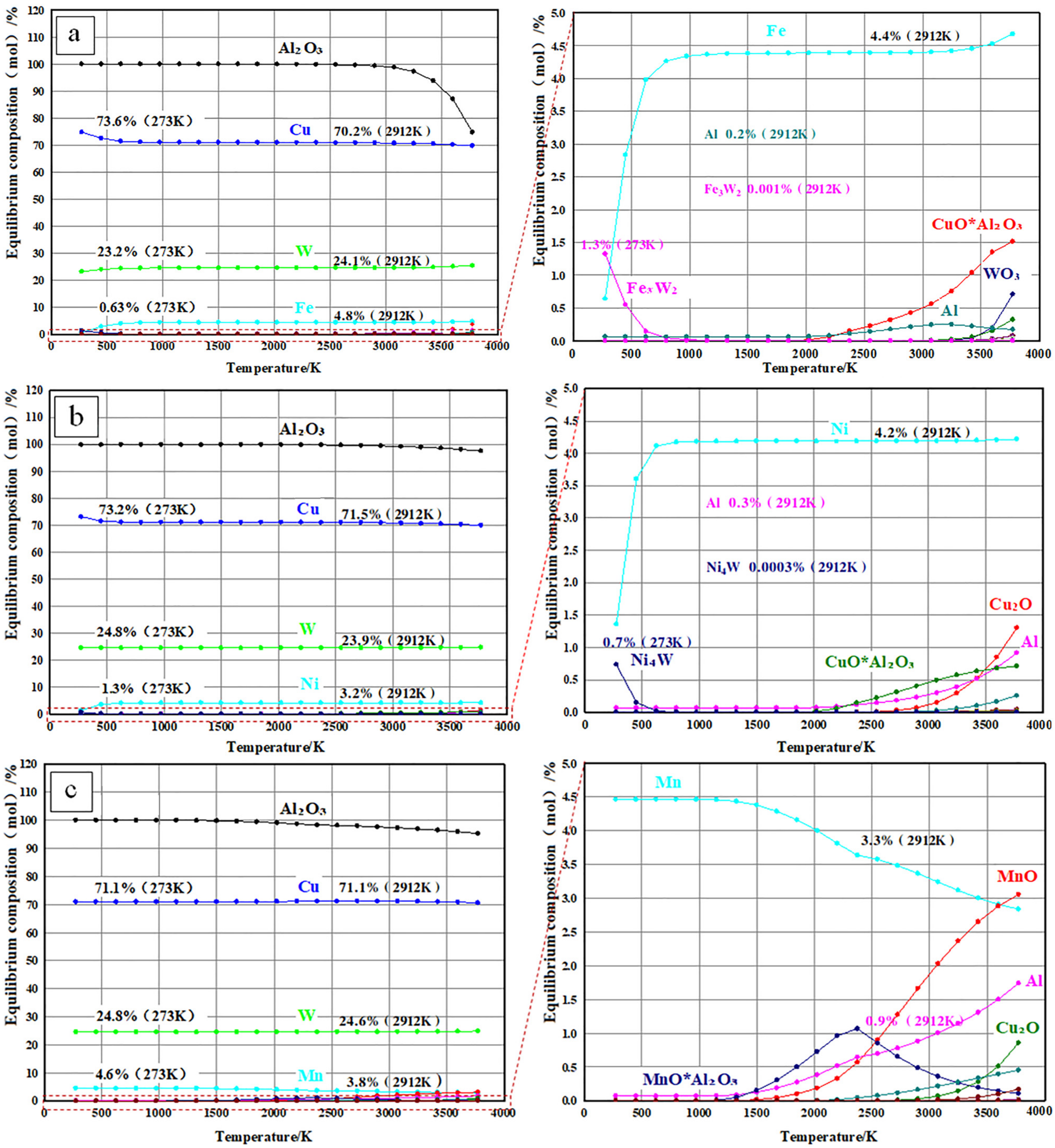

Figure 1: Thermodynamic equilibria of (a) Al–CuO–WO_3–Fe_2O_3, (b) Al–CuO–WO_3–NiO, and (c) Al–CuO–WO_3–MnO_2 systems.

calculated as 2,912, 2,902, and 2,929 K, respectively. Merzhanov [31] suggested that these systems would become self-sustaining only if $T_{ad} \geq 1,800$ K. It is thus deduced that these systems could exist.

According to the principle of minimum Gibbs free energy change, the thermodynamic equilibria of the Al–CuO–WO_3–Fe_2O_3/NiO/MnO_2 systems were calculated, and the results are shown in Figure 1. Fe_2O_3, NiO, and MnO_2 can be reduced by Al in the Al–CuO–WO_3 system to produce WCu composites microalloyed with Fe, Ni, and Mn. Moreover, Fe and Ni can combine with W to produce intermetallic compounds such as Fe_3W_2 and Ni_4W. At temperatures below 1,000 K, the mole percentages of Fe and Ni increased rapidly with increasing temperature, whereas that of Mn remained unchanged, and the Fe_3W_2 and Ni_4W contents decreased rapidly. At 1,000–2,912 K, the mole percentages of Fe and Fe_3W_2 remained stable with increasing temperature. At temperatures above 2,912 K, the mole percentage of Fe gradually increased, whereas that of Fe_3W_2 remained essentially constant. In addition, when the tem-

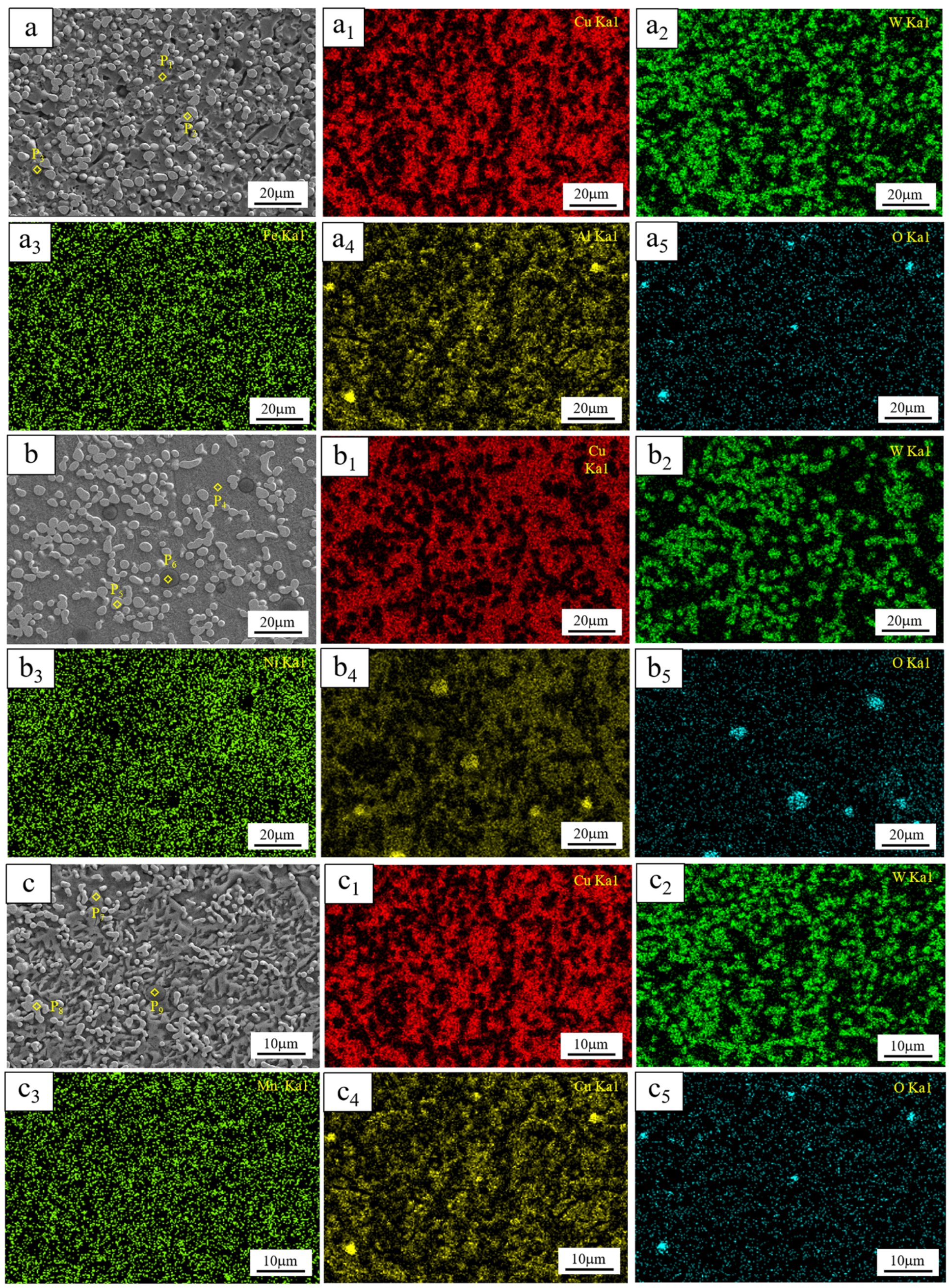

Figure 2: SEM images of WCu composites microalloyed with (a) Fe, (b) Ni, and (c) Mn, and elemental distributions of WCu composites microalloyed with (a_1–a_5) Fe, (b_1–b_5) Ni, and (c_1–c_5) Mn.

perature exceeded 2,073 K, the molar percentages of Al, CuO, and·Al_2O_3 increased gradually, which is not conducive to thermite reduction. When the temperature exceeded 1,000 K, the molar percentages of Ni and Ni_4W tended to be stable with increasing temperature. In addition, when the temperature exceeded 2,073 K, the molar percentages of Al, Cu_2O, and CuO·Al_2O_3 increased gradually, which is also not conducive to the thermite reduction reaction. At temperatures exceeding 1,000 K, the molar percentage of Mn decreased with increasing temperature, whereas those of Al, MnO, and Mn·Al_2O_3 gradually increased. Thus, high temperature is not conducive to Mn reduction. In conclusion, it is feasible to add Fe, Ni, and Mn to WCu composites *in situ* through thermite reduction.

3.2 Microalloying element characterization

Figure 2 shows the microstructure and elemental distributions of the microalloyed WCu composites.

Figure 2a–c shows that the microstructure of the microalloyed WCu composites consists mainly of a gray matrix, grayish-white tungsten particles, and black spherical inclusions. The grain boundary of the matrix (Figure 2a) is distinct, the matrix (Figure 2b) is smooth, and the matrix (Figure 2c) is heavily grooved. The elemental distributions in Figure 2a_1–a_5, b_1–b_5, and c_1–c_5 show that Cu and the microalloying elements are evenly distributed in the matrix, W is distributed on the grayish-white tungsten particles, Al is distributed mainly on the matrix and black spherical inclusions, and O is distributed mainly on the black spherical inclusions.

Figure 3 shows the EDS analysis of phases P_1–P_9 in Figure 2a–c. The results for P_1, P_4, and P_7 show that Ni, Fe, and Mn were dissolved in the copper matrix, and their content decreased in turn, while the content of aluminum in the matrix increased. The thermodynamic equilibria in Figure 1 show that at 1,800–3,000 K, the Ni and Fe contents remained essentially stable, and the Al content increased with increasing temperature, whereas the Mn content decreased gradually. These values are in good agreement with the experimental results. The results for P_2, P_5, and P_8 show that the grayish-white tungsten particles contained only W. The results for P_3, P_6, and P_9 show that the atomic ratio of Ca, Al, and O in the black

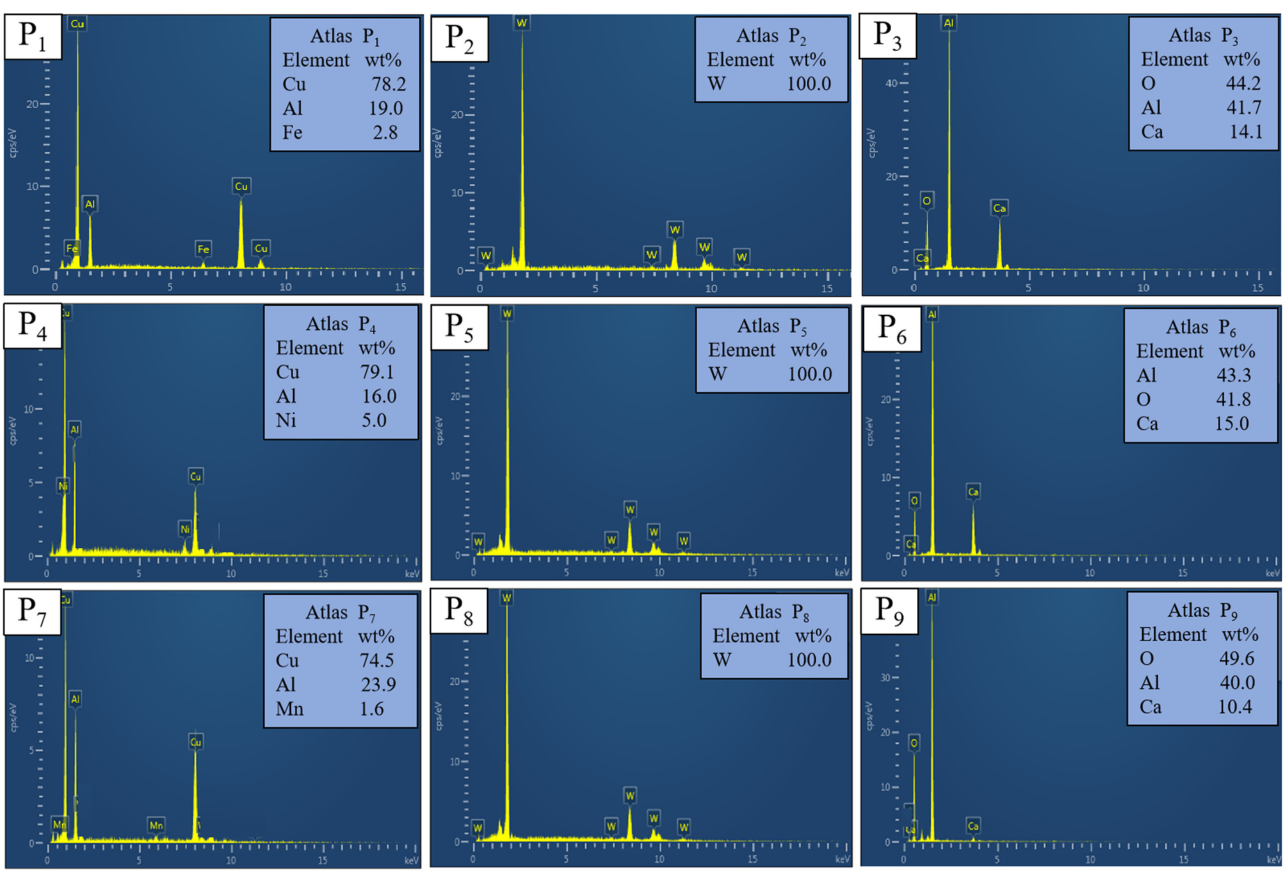

Figure 3: EDS analysis of Point (P_1–P_9) in Figure 2.

Table 1: Composition of microalloyed WCu composites

Element	W	Al	O	Ca	Fe	Ni	Mn	Cu
Fe	43.46	7.25	2.65	0.27	1.53	—	—	Bal.
Ni	44.64	8.36	3.92	0.36	—	2.86	—	Bal.
Mn	38.49	12.21	3.72	0.23	—	—	0.70	Bal.

spherical inclusions was close to 1:4:7, indicating that the inclusions were $CaAl_4O_7$.

Table 1 shows the chemical compositions of the microalloyed WCu composites. The Ni, Fe, and Mn contents in the microalloyed WCu composites are lower than the target content of 3.0 wt%. The Ni yield is the highest (95.33%), possibly because Ni is infinitely soluble in copper, and Ni can combine with W to form Ni_4W (as shown in Figure 1), which promotes the forward chemical reaction. The Fe yield is 51.00%; the main reason may be the low solubility of Fe in copper. The yield of Mn is the lowest, only 23.33%; the main reason is that the high temperature during SHS is not conducive to the forward process of the reduction reaction, in which MnO_2 is reduced by Al. This result is consistent with the results in Figure 1. Ca and O were present in the WCu composites mainly in inclusions consisting of Ca, Al, and O. The Al content included solid-solution Al in the matrix and the Al in inclusions.

3.3 Tungsten particle characteristics

Figure 4 shows the phase distributions of the microstructure in the microalloyed WCu composites.

The phase area ratio of tungsten particles in the Ni-containing WCu composite is the largest (34.35%), followed by those of the Fe-containing composite (24.78%) and the Mn-containing composite (24.12%). These values are associated mainly with the tungsten content of the microalloyed WCu composites. The phase area ratios of

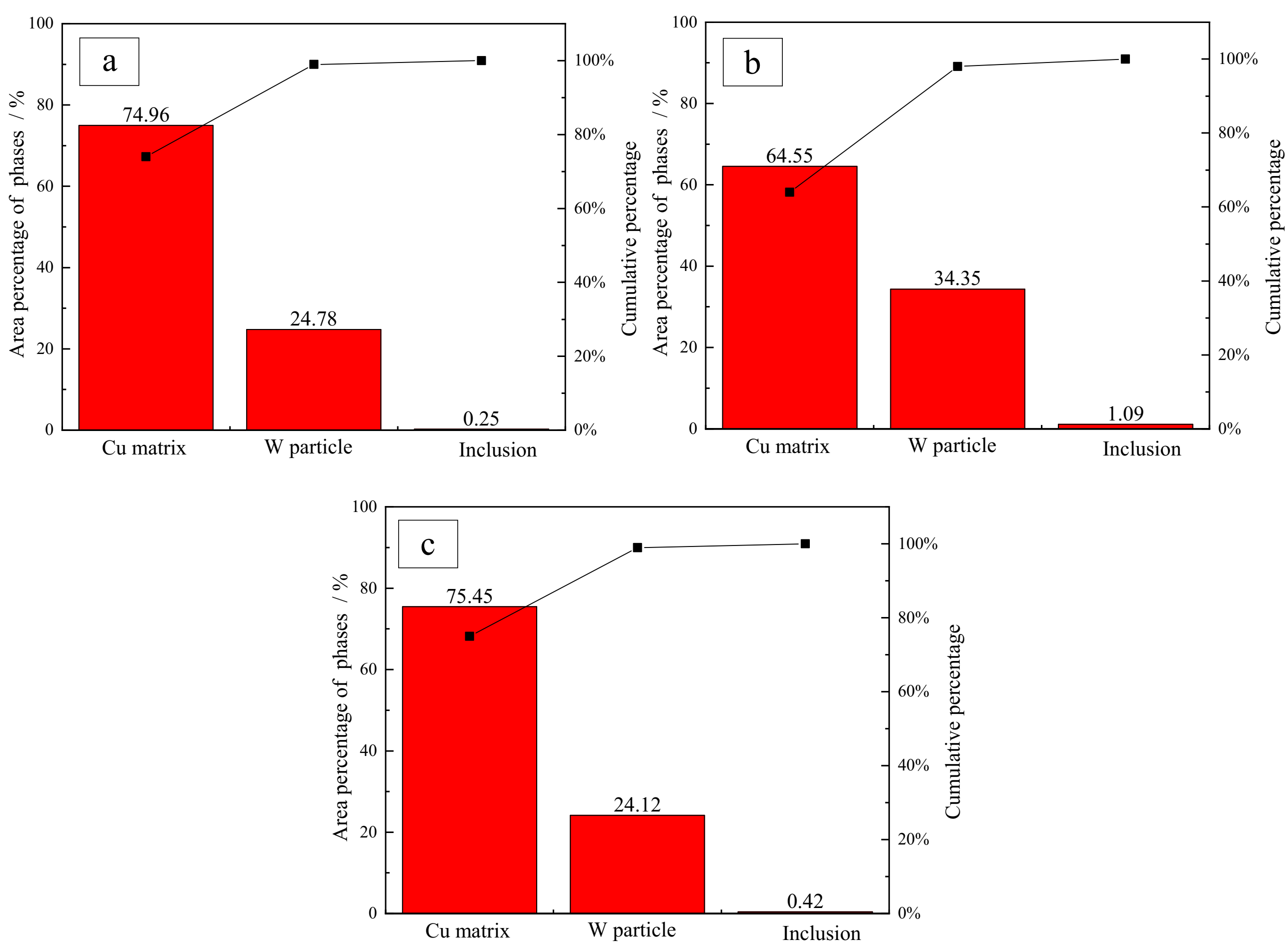

Figure 4: Phase distributions of microstructure in WCu composites microalloyed with (a) Fe, (b) Ni, and (c) Mn.

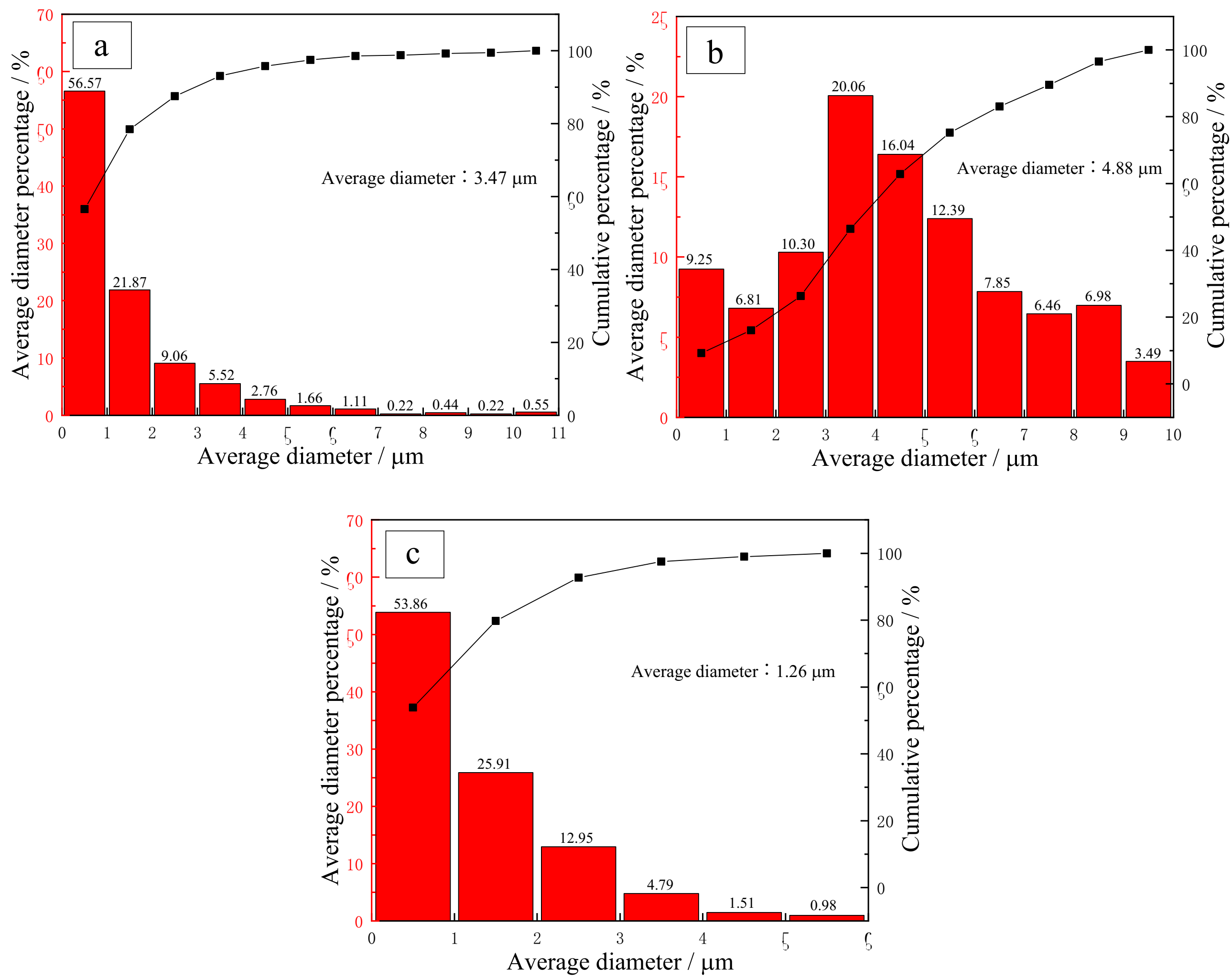

Figure 5: W particle distributions in microstructure of WCu composites microalloyed with (a) Fe, (b) Ni, and (c) Mn.

inclusions in the WCu composites microalloyed with Fe, Ni, and Mn are 0.25, 1.09, and 0.42%, respectively. These results are consistent with the variation of the tungsten and oxygen contents in Table 1.

Figure 5 shows the W particle distributions in the microstructure of the microalloyed WCu composites. The average diameters of W particles in the WCu composites microalloyed with Fe, Ni, and Mn are 3.47, 4.88, and 1.26 μm, respectively. Mn clearly decreases the size of tungsten particles, and the size reduction effect of the microalloying elements on tungsten particles follows the order Mn > Fe > Ni. The tungsten particle size of the Fe-containing WCu composite ranges from 0 to 11.00 μm but the size is concentrated at 0–2.00 μm; the particle size of the Ni-containing WCu composite ranges from 0 to 10.00 μm but the size is distributed discretely; and the particle size of the Mn-containing WCu composite ranges from 0 to 6.00 μm but the size is concentrated at 0–2.00 μm.

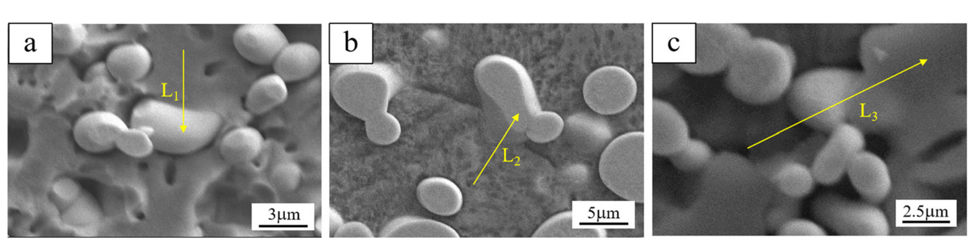

Figure 6: Typical W/Cu interface in microstructures of WCu composites microalloyed with (a) Fe, (b) Ni, and (c) Mn.

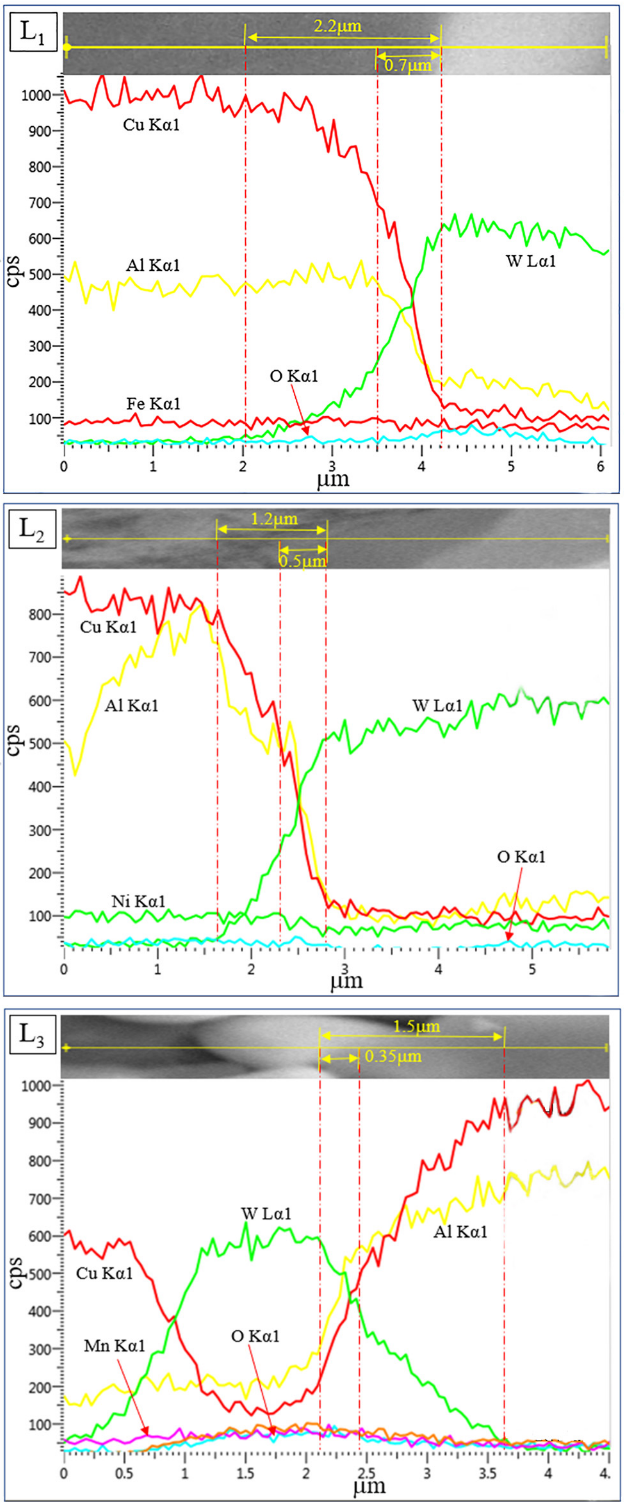

Figure 7: Line scan analysis of typical W/Cu interfaces in Figure 6 (L_1: Fe, L_2: Ni, and L_3: Mn).

These results indicate that the tungsten particles have a more uniform size when the microalloying element has a greater size reduction effect on tungsten particles.

3.4 Interface behavior

Figure 6 shows that there is no obvious phase interface between tungsten particles and the matrix with the microalloying elements. In addition, the matrices of the WCu composites microalloyed with Fe and Mn are relatively smooth, whereas that of the composite microalloyed with Ni appears fuzzy and the fuzziness may strengthen the W/Cu interface.

Figure 7 shows line scan analyses of typical W/Cu interfaces. A transition zone clearly appears between tungsten particles and the copper matrix. Along the scanning direction, the Cu, Al, and microalloying element contents decrease gradually, whereas the W content increases gradually. Here, d_1 and d_2 are defined as the interfacial transition zone, in which the Cu and W contents and the Al and microalloying element contents, respectively, change at the W/Cu interface. The thicknesses (d_1) of the WCu composites microalloyed with Fe, Ni, and Mn are 2.2, 1.2, and 1.5 μm, respectively. This result indicates that each microalloying element reduces the surface tension of the liquid metal to a different degree, and the effect on the wettability of the interface follows the order Ni > Mn > Fe. The thicknesses (d_2) of the WCu composites microalloyed with Fe, Ni, and Mn are 0.7, 0.5, and 0.35 μm, respectively. This result indicates that the thickness of the intermetallic compound layer or solid solution layer of the microalloying element at the W/Cu interface follows the order Fe > Ni > Mn. According to the results in Figure 1, the intermetallic compounds Fe_3W_2 and Ni_4W are typically produced at the W/Cu interface of the WCu composites microalloyed with Fe and Ni, whereas a solid solution layer is typically produced at that of the composite microalloyed with Mn [32].

4 Conclusion

Fe, Ni, and Mn can be added to WCu composites *in situ* by thermite reduction. Below the adiabatic temperature, the increasing temperature has little effect on the reduction of Fe_2O_3 and NiO by Al but is not conducive to the reduction of MnO_2 by Al. The content of the microalloying elements in the microalloyed WCu composites was below the target value. The yields of Ni, Fe, and Mn followed the order Ni > Fe > Mn. The microalloying elements Ni, Fe, and Mn were solidly dissolved in the copper matrix, and their contents decreases in turn, while the Al content in the matrix increased. Mn clearly reduced the size of tungsten particles, and the size reduction effect of the microalloying elements on tungsten particles followed the order Mn > Fe > Ni. The effect on the wettability of the interface followed the order Ni > Mn > Fe. The intermetallic compounds Fe_3W_2 and Ni_4W were typically produced at the W/Cu interface of the WCu composites microalloyed with Fe and Ni, whereas a solid solution layer was typically produced on the composite microalloyed with Mn. Increasing interfacial wetting was not conducive to the reduction of the tungsten particle size.

Funding Information: This research was supported by the Key Scientific Research Project of colleges and universities of Henan Province (Grant No. 22A450002), Key Technologies R & D Program of Henan Province (Grant No. 202102210207), Chinese Postdoctoral Science Foundation (Grant No. 2020M672222), Doctoral Scientific Research Foundation of Henan University of Science and Technology (Grant No. 13480091), and Postdoctoral Scientific Research Foundation of Henan University of Science and Technology (Grant No. 13554020).

Author contributions: All authors have accepted responsibility for the entire content of this manuscript and approved its submission.

Conflict of interest: The authors state no conflict of interest.

References

[1] Madhur V, Srikanth M, Annamalai AR, Muthuchamy A, Jen CP. Effect of nano copper on the densification of spark plasma sintered W-Cu composites. Nanomater. 2021;11(2):413.
[2] Zhang X, Zhang Y, Tian B, Jia Y, Liu Y, Song K, et al. Cr Effects on the electrical contact properties of the Al_2O_3-Cu/15W composites. Nanotechnol Rev. 2019;8(1):128–35.
[3] Zhang XH, Zhang Y, Tian BH, Jia YL, Liu Y, Song KX, et al. Arc erosion behavior of TiB_2/Cu composites with single-scale and dual-scale TiB_2 particles. Nanotechnol Rev. 2019;8(1):619–27.
[4] Dong LL, Chen WG, Zheng CH, Deng N. Microstructure and properties characterization of tungsten–copper composite materials doped with graphene. J Alloy Compd. 2017;695:1637–46.
[5] Krauss W, Lorenz J, Konys J, Gaganidze E. Mechanical characterization of electrochemically based W-Cu joints for low-temperature heat sink application. Fusion Eng Des. 2017;124:220–5.
[6] Xu L, Srinivasakannan C, Zhang LB, Yan M, Peng JH, Xia HG, et al. Fabrication of tungsten-copper alloys by microwave hot pressing sintering. J Alloy Compd. 2016;658(15):23–8.
[7] Wang YL, Zhuo LC, Yin EH. Progress, challenges and potentials/trends of tungsten-copper (W Cu) composites/pseudo-alloys: Fabrication, regulation and application. Int J Refract Met Hard Mater. 2021;100:105648.
[8] Echlin MP, Mottura A, Wang M, Mignone PJ, Riley DP, Franks GV, et al. Three-dimensional characterization of the permeability of W-Cu composites using a new "Tribeam" technique. Acta Mater. 2014;64:307–15.
[9] Feng J, Liang SH, Guo XH, Zhang Y, Song KX. Electrical conductivity anisotropy of copper matrix composites reinforced with SiC whiskers. Nanotechnol Rev. 2019;8(1):285–92.
[10] Zhang XH, Zhang Y, Tian BH, Song KX, Liu P, Jia YL, et al. Review of nano-phase effects in high strength and conductivity copper alloys. Nanotechnol Rev. 2019;8(1):383–95.
[11] Zhao MY, Inas I, Pfeifenberger MJ, Wurmshuber M, Kiener D. Tailoring ultra-strong nanocrystalline tungsten nanofoams by reverse phase dissolution. Acta Mater. 2020;182:215–25.
[12] Zhang Y, Tan G, Zhang MY, Yu Q, Liu ZQ, Liu YY, et al. Bioinspired tungsten-copper composites with bouligand-type architectures mimicking fish scales. J Mater Sci Technol. 2022;96(10):21–30.
[13] Yao GC, Pan SH, Yuan J, Guan Z, Li XC. A novel process for manufacturing copper with size-controlled in-situ tungsten nanoparticles by casting. J Mater Process Technol. 2021;296:117187.
[14] Lu TX, Chen CG, Li P, Zhang CZ, Han WH, Zhou Y, et al. Enhanced mechanical and electrical properties of in situ synthesized nano-tungsten dispersion-strengthened copper alloy. Mater Sci Eng A. 2021;799:140161.
[15] Wang X, Zhang X, Zhao L, Zhao C, Zhang H, Du Y, et al. Tungsten/copper composite sheets prepared by a novel encapsulation rolling technique. J Alloy Compd. 2021;884(5):161051.
[16] Johnson JL, German RM. Phase equilibria effects on the enhanced liquid phase sintering of tungsten-copper. Metall Trans A. 1993;24(11):2369–77.
[17] Cao WC, Liang SH, Gao ZF, Wang XH, Yang XH. Effect of Fe on vacuum breakdown properties of CuW alloys. Int J Refract Met Hard Mater. 2011;29(6):656–61.
[18] Yang XH, Xiao P, Liang SH, Zou JT, Fan ZK. Alloying effect of Ni and Cr on the wettability of copper on W substrate. Acta Metall Sin. 2008;21(5):369–79.
[19] Wang C, Liang SH, Cao F, Zhang Q. Interface microstructure evolution of a novel CuW/Al composite fabricated by an infiltration method. J Alloy Compd. 2020;816:152506.
[20] Bai YX, Liang SH, Wang XH. Simulation on the infiltration with insufficience of molten Cu into W micro-channel. Int J Refract Met Hard Mater. 2015;50(5):100–5.
[21] Coester B, Wong G, Xu Z, Tang J, Gan WL, Lew WS. Enhanced spin Hall conductivity in tungsten-copper alloys. J Magn Magn Mater. 2021;523:167545.
[22] Zhuo LC, Zhang JL, Zhang QQ, Wang HL, Zhao Z, Chen QY, et al. Achieving both high conductivity and reliable high strength for W-Cu composite alloys using spherical initial powders. Vac. 2020;181:109620.
[23] He G, Zhao P, Guo SB, Chen YX, Liu GH, Li JT. In suit synthesis and bonding of Cu to W–Cu composite by combustion synthesis and centrifugal infiltration. J Alloy Compd. 2013;579:71–4.
[24] Guo YJ, Guo HT, Gao BX, Wang XG, Hu YB, Shi ZQ. Rapid consolidation of ultrafine grained W-30 wt% Cu composites by

field assisted sintering from the sol-gel prepared nanopowders. J Alloy Compd. 2017;724:155–62.
[25] Zhang YH, Zhuo LC, Zhao Z, Zhang QQ, Zhang JL, Liang SH, et al. The influence of pre-sintering temperature on the microstructure and properties of infiltrated ultrafine-grained tungsten-copper composites. J Alloy Compd. 2020;823(15):153761.
[26] Cheng C, Dou ZH, Zhang TA, Song YL. Multistage desulfurization mechanism to reduce sulfur content of high ferrotitanium prepared using thermite method. Rare Met. 2021;40:2313–9.
[27] Cheng C, Dou ZH, Zhang TA, Su JM, Liu Y, Niu LP. Sulfur distribution in preparation of high titanium ferroalloy by thermite method with different CaO additions. Rare Met. 2019;38(08):793–81.
[28] Cheng C, Dou ZH, Zhang TA, Su JM, Niu LP. Distribution and control mechanism of Al and O residuals in ferrotitanium prepared by aluminothermic reduction with insufficient Al. JOM. 2019;71:809–14.
[29] Cheng C, Dou ZH, Zhang TA. Formation mechanism and distribution of Al and O in the ferrotitanium with different Ti contents prepared by thermite method. JOM. 2019;71(10):3584–9.
[30] Cheng C, Song KX, Mi XJ, Wu BA, Xiao Z, Xie HF, et al. Microstructural evolution and properties of Cu-20 wt% Ag alloy wire by multi-pass continuous drawing. Nanotechnol Rev. 2020;9(1):1359–67.
[31] Merzhanov AG. The chemistry of self-propagating high-temperature synthesis. J Mater Chem. 2004;18:7766–9.
[32] Yang XH, Fan ZK, Liang SH, Peng X. Effects of Fe on wetting behaviors and interfacial characteristics between copper alloy and W substrate. Trans Nonferrous Met Soc China. 2009;19(1):153–9.